

# CHAPTER 105

## TOTAL WAVE FORCE ON A VERTICAL CIRCULAR CYLINDRICAL PILE

Yoshito Tsuchiya  
Professor of Coastal Engineering

and

Masataka Yamaguchi  
Assistant Professor of Coastal Engineering  
Disaster Prevention Research Institute, Kyoto University  
Kyoto, Japan

### ABSTRACT

This paper deals with the estimation of total wave force on a vertical circular cylindrical pile. Firstly, finite amplitude wave theories such as those of Stokes waves and cnoidal waves are recalculated by the Stokes second definition of wave celerity and the applicability of the theories for wave crest height above the still water level, wave celerity and horizontal water particle velocity is briefly discussed. Secondly, the drag and inertia coefficients are estimated respectively from the results of experiments for total wave force by the authors and by other researchers, based on the Morison wave force equation applying the theories and characteristics of the coefficients are considered in relation to the wave characteristics and pile dimension. Lastly, the applicability of the wave force equation proposed is investigated in comparison with experimental and theoretical results for time variation of total wave force and maximum total wave force.

### INTRODUCTION

It is needless to say that accurate estimation of wave force on ocean structures in the design is of very importance. In present state, the two methods as a practical approach are usually used for the estimation of wave force acting on a rigid circular cylindrical pile by nonbreaking waves. The one is based on the theory of wave diffraction (MacCamy-Fuchs, 1954 and Yamaguchi-Tsuchiya, 1974) of which solution is obtained from the boundary value problem under the assumption of inviscid fluid and irrotational motion. The other is the so-called Morison wave force equation (Morison, 1950) which expresses each component of wave force divided into the drag force and the inertia force with characteristics of incident waves, assuming that the wave motion is not essentially disturbed by the existence of the pile.

It is important factors in calculating the wave force by the Morison wave force equation to estimate accurately the wave crest height above the still water level, water particle velocity and water particle acceleration and to select properly the drag and inertia coefficients.

In this paper, from this point of view, some examinations are made. Based on the finite amplitude wave theories and the wave-pile characteristics, a relation between the drag and inertia coefficients estimated from many exper-

imental results is established as well as the applicability of the theories to the wave force equation. Also, the validity of the wave force equation proposed is examined comparing the theoretical results of total wave force with the experimental ones. In this investigation, the total wave force on a pile by non-breaking finite amplitude waves is discussed under the assumption that the diameter of pile is small compared with the wave length and consequently the effect of wave diffraction by the pile on the total wave force can be neglected.

FINITE AMPLITUDE WAVE THEORIES AND WAVE FORCE EQUATION

(1) Finite Amplitude Wave Theories (Tsuchiya-Yamaguchi, 1972) For the estimation of wave force, there are many fruitful theories of finite amplitude waves such as Stokes waves and cnoidal waves. The wave theories however have been derived by using either of two physical definitions of wave celerity (Stokes, 1880). The one is the so-called Stokes first definition of wave celerity, which means that the average horizontal water particle velocity over a wave length is vanished, and it is given as

$$c = \frac{\int_0^L (c + u) dx}{\int_0^L dx} \dots\dots\dots (1)$$

in which c is the wave celerity, L the wave length, u the horizontal water particle velocity and x the horizontal coordinate at the still water level. The other is the Stokes second definition, which is given as

$$c = \frac{\int_0^L \int_{-h}^{\eta} (c + u) dz dx}{\int_0^L \int_{-h}^{\eta} dz dx} \dots\dots\dots (2)$$

in which h is the depth of water, η the surface displacement from the still water level and z the vertical coordinate being taken positive upward from the still water level. According to this definition, the average momentum over a wave length is vanished by addition of a uniform motion.

Table 1 shows a classification of such wave theories by the definition of wave celerity. For the analytical solution of Stokes waves, there are so many theories, but they all use the first definition. On the contrary, for the cnoidal waves, there are three theories; the Chappellear theory is derived by the first definition and the others are done by the second one. In this section, the Stokes wave theory by Skjelbreia and Hendrickson (1960) and the cnoidal wave theory by Chappellear (1962) are recalculated using the second definition.

If the moving coordinate system with the wave celerity as shown in Fig. 1 is used for an irrotational steady periodic waves and the dimensionless quantities are defined by

$$\left. \begin{aligned} \bar{\phi} &= \frac{k\phi}{c\lambda}, \quad \bar{X} = kX, \quad \bar{z} = kz, \quad \bar{\eta} = \frac{k\eta}{\lambda}, \quad \bar{h} = kh, \quad \bar{c} = \sqrt{\frac{k}{g}} c \\ \bar{Q} &= \frac{kQ}{\lambda^2}, \quad \bar{u} = \frac{u}{c\lambda}, \quad \bar{w} = \frac{w}{c\lambda} \end{aligned} \right\} \dots\dots\dots (3)$$

the basic equation can be expressed as

$$\frac{\partial^2 \bar{\phi}}{\partial \bar{X}^2} + \frac{\partial^2 \bar{\phi}}{\partial \bar{z}^2} = 0 \dots\dots\dots (4)$$

in which φ the velocity potential, k the wave number, λ a small expansion para-

Table 1 Classification of finite amplitude wave theories by the definition of wave celerity

Wave Theory	Definition of Wave Celerity	
	The first definition	The second definition
Analytical solution (Stokes waves)	Stokes (2nd approx., 1880) Tanaka (3rd approx., 1953) De (5th approx., 1955) Skjelbreia (3rd approx., 1959) Skjelbreia & Hendrickson (5th approx., 1960) Bretschneider (5th approx., 1960)	Authors (4th approx., 1972)
Analytical solution (Cnoidal waves)	Chappellear (3rd approx., 1962)	Keulegan & Patterson (1st approx., 1940) Laitone (2nd approx., 1961) Authors (3rd approx., 1972)
Numerical solution (Stokes waves)	Chappellear (1961) Dean (1965)	von Schwind & Reid (1972)

meter which will be determined later,  $g$  the acceleration of gravity,  $Q$  the Bernoulli constant,  $w$  the vertical water particle velocity and  $X$  the abscissa in the steady state coordinate system. The dimensionless velocity potential  $\bar{\phi}$  is defined as

$$\bar{u} = \frac{\partial \bar{\phi}}{\partial \bar{X}}, \quad \bar{w} = \frac{\partial \bar{\phi}}{\partial \bar{z}} \dots \dots \dots (5)$$

The boundary conditions at the bottom and at the water surface are given respectively as

$$\frac{\partial \bar{\phi}}{\partial \bar{z}} = 0; \quad \bar{z} = -\bar{h} \dots \dots \dots (6)$$

$$\frac{\partial \bar{\phi}}{\partial \bar{z}} + \frac{\partial \bar{\eta}}{\partial \bar{X}} - \lambda \frac{\partial \bar{\eta}}{\partial \bar{X}} \frac{\partial \bar{\phi}}{\partial \bar{X}} = 0; \quad \bar{z} = \lambda \bar{\eta} \dots \dots \dots (7)$$

$$-\bar{c}^2 \frac{\partial \bar{\phi}}{\partial \bar{X}} + \bar{\eta} + \lambda \left[ \frac{1}{2} \bar{c}^2 \left\{ \left( \frac{\partial \bar{\phi}}{\partial \bar{X}} \right)^2 + \left( \frac{\partial \bar{\phi}}{\partial \bar{z}} \right)^2 \right\} + \bar{Q} \right] = 0; \quad \bar{z} = \lambda \bar{\eta} \dots \dots \dots (8)$$

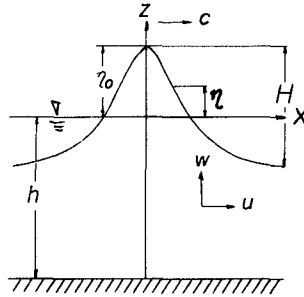


Fig. 1 Definition sketch of coordinate system used

The perturbation method is able to be applied in order to obtain the approximate solution, as a small parameter  $\lambda$  is included in the above equations. According to the perturbation method of Skjelbreia and Hendrickson, the velocity potential in a series form satisfying the Laplace equation and the boundary condition at the bottom as well as the corresponding wave profile are assumed to the fourth order approximation as follows:

$$\bar{\phi} = (A_{01} + \lambda A_{02} + \lambda^2 A_{03} + \lambda^3 A_{04}) \bar{X} + (A_{11} + \lambda^2 A_{12}) \cosh(\bar{h} + \bar{z}) \sin \bar{X} + (\lambda A_{22} + \lambda^3 A_{24}) \cosh 2(\bar{h} + \bar{z}) \sin 2\bar{X} + \lambda^2 A_{33} \cosh 3(\bar{h} + \bar{z}) \sin 3\bar{X} + \lambda^3 A_{44} \cosh 4(\bar{h} + \bar{z}) \sin 4\bar{X} \dots (9)$$

$$\bar{\eta} = \cos \bar{X} + (\lambda B_{22} + \lambda^3 B_{24}) \cos 2\bar{X} + \lambda^2 B_{33} \cos 3\bar{X} + \lambda^3 B_{44} \cos 4\bar{X} \dots \dots \dots (10)$$

in which  $A_{ij}$  and  $B_{ij}$  are the coefficients to be determined. The first term in Eq. (9) being also  $i, j$  harmonic function is different from the assumption by Skjelbreia and Hendrickson as already pointed out by Stokes (1880). Furthermore, the following equations are assumed for the Bernoulli constant and the wave celerity

$$\bar{Q} = C_3 + \lambda^2 C_4 \dots\dots\dots (11)$$

$$\bar{c}^2 = C_0^2 (1 + \lambda^2 C_1) \dots\dots\dots (12)$$

in which  $C_1$  is the coefficient to be determined.

If Eqs. (9), (10), (11) and (12) are substituted into a set of the boundary condition at the free surface, Eqs. (7) and (8), the coefficients  $A_{ij}$ ,  $B_{ij}$  and  $C_i$  are determined from the grouped powers of  $\lambda$  and sub-grouped powers  $i_j$  of  $\cos(nX)$  and  $\sin(nX)$  according to the procedure of Skjelbreia and Hendrickson. The coefficients are finally determined as

$$\left. \begin{aligned} A_{01} = 0, \quad A_{03} = 0, \quad A_{11} &= \frac{1}{\sinh kh}, \quad A_{13} = -\frac{(5 \cosh^2 kh + 1) \cosh^2 kh}{8 \sinh^5 kh} - \frac{A_{02}}{\sinh kh} \\ A_{22} &= \frac{3}{8 \sinh^4 kh}, \quad A_{24} = \frac{192 \cosh^8 kh - 424 \cosh^6 kh - 312 \cosh^4 kh + 480 \cosh^2 kh - 17}{768 \sinh^{10} kh} \\ &- \frac{3 A_{02}}{8 \sinh^4 kh}, \quad A_{33} = \frac{-4 \cosh^2 kh + 13}{64 \sinh^7 kh} \\ A_{44} &= \frac{80 \cosh^6 kh - 816 \cosh^4 kh + 1338 \cosh^2 kh - 197}{1536 (-1 + 6 \cosh^2 kh) \sinh^{10} kh} \end{aligned} \right\} \dots (13)$$

$$\left. \begin{aligned} B_{22} &= \frac{(2 \cosh^2 kh + 1) \cosh kh}{4 \sinh^3 kh} \\ B_{24} &= \frac{272 \cosh^9 kh - 504 \cosh^7 kh - 192 \cosh^5 kh + 322 \cosh^3 kh + 21 \cosh kh}{384 \sinh^9 kh} \\ B_{33} &= \frac{24 \cosh^6 kh + 3}{64 \sinh^6 kh} \\ B_{44} &= \frac{768 \cosh^{11} kh - 448 \cosh^9 kh - 48 \cosh^7 kh + 48 \cosh^5 kh + 106 \cosh^3 kh - 21 \cosh kh}{384 (6 \cosh^2 kh - 1) \sinh^9 kh} \end{aligned} \right\} \dots (14)$$

$$\left. \begin{aligned} C_0^2 &= \tanh kh, \quad C_1 = \frac{8 \cosh^4 kh - 8 \cosh^2 kh + 9}{8 \sinh^4 kh} + 2 A_{02} \\ C_3 &= -\frac{1}{4 \sinh kh \cosh kh} + \frac{\sinh kh}{\cosh kh} A_{02} \\ C_4 &= \frac{4 \cosh^6 kh + 16 \cosh^4 kh - 38 \cosh^2 kh + 9}{64 \sinh^7 kh \cosh kh} + \frac{4 \cosh^4 kh + 5}{8 \sinh^3 kh \cosh kh} A_{02} \\ &+ \frac{2 \sinh kh}{\cosh kh} A_{02}^2 + \frac{\sinh kh}{\cosh kh} A_{01} \end{aligned} \right\} \dots (15)$$

The above formulation by the authors coincides with the one by Skjelbreia and Hendrickson, if the terms of  $A_{02}$  and  $A_{04}$  are vanished.

Applying the Stokes second definition of wave celerity expressed by Eq. (2) to determine the coefficients  $A_{02}$  and  $A_{04}$ , the calculation finally yields

$$\left. \begin{aligned} A_{02} &= -\frac{\cosh kh}{2 kh \sinh kh} \\ A_{04} &= \frac{4 \cosh^7 kh - 20 \cosh^5 kh + 16 \cosh^3 kh - 9 \cosh kh}{32 kh \sinh^7 kh} - \left( \frac{\cosh kh}{2 kh \sinh kh} \right)^2 \end{aligned} \right\} \dots\dots\dots (16)$$

Therefore, the wave celerity and the horizontal and vertical water particle velocities are written respectively as

$$\frac{c}{\sqrt{gh}} = \sqrt{\frac{\tanh kh}{kh} (1 + \lambda^2 C_1)} \dots\dots\dots (17)$$

$$\frac{u}{c} = \lambda^2 A_{02} + \lambda^4 A_{04} + (\lambda A_{11} + \lambda^3 A_{13}) \cosh h(h+z) \cos kX + 2(\lambda^2 A_{22} + \lambda^4 A_{24}) \cosh 2k(h+z) \cos 2kX + 3\lambda^3 A_{33} \cosh 3k(h+z) \cos 3kX + 4\lambda^4 A_{44} \cosh 4k(h+z) \cos 4kX \dots\dots\dots (18)$$

$$\frac{w}{c} = (\lambda A_{11} + \lambda^3 A_{13}) \sinh k(h+z) \sin kX + 2(\lambda^2 A_{22} + \lambda^4 A_{24}) \sinh 2k(h+z) \sin 2kX + 3\lambda^3 A_{33} \sinh 3k(h+z) \sin 3kX + 4\lambda^4 A_{44} \sinh 4k(h+z) \sin 4kX \dots\dots\dots (19)$$

The small parameter  $\lambda$  is also expressed as

$$2(\lambda + \lambda^3 B_{33}) = kH \dots\dots\dots (20)$$

in which H is the wave height. It is apparent from the definition of wave celerity that the wave celerity by both the definitions coincides in deep water waves. The horizontal water particle velocity corresponds to the one to be superposed the steady current of higher order term in the wave theory, in which the average mass transport vanishes, on the periodic motion of water particle.

On the other hand, the Chappellear cnoidal wave theory by the first definition to the third approximation is transformed into the theory by the second definition, if only substituting the expressions for horizontal water particle velocity and surface profile into Eq. (2) through a tedious calculation. The calculation yields

$$\left. \begin{aligned} \frac{c}{\sqrt{gh}} = & 1 + (L_3 + L_0 \kappa^2 S_1) + \left[ -\frac{1}{4} L_0^2 \kappa^2 + \left\{ 5L_0 L_3 \kappa^2 + \frac{3}{2} L_0^2 \kappa^2 (1 + \kappa^2) \right\} S_1 \right. \\ & - \frac{3}{4} L_0^2 \kappa^4 S_2 + L_0^2 \kappa^4 S_1^2 \left. \right] + \left[ -\frac{63}{80} L_0^3 \kappa^2 (1 + \kappa^2) - \frac{9}{4} L_0^3 L_3 \kappa^2 + \left\{ 10L_0 L_3^2 \kappa^2 \right. \right. \\ & + \frac{27}{2} L_0^2 L_3 \kappa^2 (1 + \kappa^2) + \frac{12}{5} L_0^3 \kappa^2 (1 + \kappa^2)^2 + \frac{1}{80} L_0^3 \kappa^2 (46 + 119\kappa^2 \\ & + 46\kappa^4) \left. \right\} S_1 + \left\{ -\frac{27}{4} L_0^2 L_3 \kappa^4 - \frac{241}{80} L_0^3 \kappa^4 (1 + \kappa^2) \right\} S_2 + \frac{101}{80} L_0^3 \kappa^4 S_3 \\ & + \left. \left\{ 9L_0^2 L_3 \kappa^4 + 3L_0^3 \kappa^4 (1 + \kappa^2) \right\} S_1^2 - \frac{3}{2} L_0^3 \kappa^6 S_1 S_2 + L_0^3 \kappa^6 S_1^3 \right] \end{aligned} \right\} \dots\dots\dots (21)$$

in which  $\kappa$  is the modulus of Jacobian elliptic function,  $L_0$  and  $L_3$  the expansion parameters which are calculated from the following equation for the second approximation.

$$\left. \begin{aligned} \frac{H}{h} = & \kappa^2 L_0 \left\{ 1 + \frac{1}{4} L_0 (10 + 7\kappa^2) + 6L_3 \right\} \\ & 2L_3 + L_0 \left( \kappa^2 + \frac{E}{K} \right) + L_0^2 \left\{ -\frac{1}{5} (1 - 6\kappa^2 - 9\kappa^4) + 2(1 + \kappa^2) \frac{E}{K} \right\} + 6L_0 L_3 \left( \kappa^2 + \frac{E}{K} \right) + L_3^2 = 0 \end{aligned} \right\} \dots (22)$$

And  $S_1$ ,  $S_2$  and  $S_3$  are given as

$$\left. \begin{aligned} S_1 = & \frac{1}{L} \int_0^L \sin^2 \left( \frac{\sqrt{3} L_0}{2h} X \right) dX = \frac{1}{\kappa^2} \left( 1 - \frac{E}{K} \right) \\ S_2 = & \frac{1}{L} \int_0^L \sin^4 \left( \frac{\sqrt{3} L_0}{2h} X \right) dX = \frac{1}{3\kappa^4} \left\{ -2(1 + \kappa^2) \frac{E}{K} + \kappa^2 + 2 \right\} \\ S_3 = & \frac{1}{L} \int_0^L \sin^6 \left( \frac{\sqrt{3} L_0}{2h} X \right) dX = \frac{1}{15\kappa^6} \left\{ (-8\kappa^4 - 7\kappa^2 - 8) \frac{E}{K} + 4\kappa^4 + 3\kappa^2 + 8 \right\} \end{aligned} \right\} \dots\dots\dots (23)$$

in which K and E are the complete elliptic integrals of the first and the second kind respectively. In the limiting case where  $\kappa = 1$ , the cnoidal waves become the solitary wave and the wave celerity by both the definitions coincides as

$$\frac{c}{\sqrt{gh}} = 1 + (L_3 + L_0) + (3L_0^2 + 5L_0L_3) + (10L_0L_3^2 + 27L_0^2L_3 + \frac{57}{5}L_0^3) \dots \dots \dots (24)$$

The other wave characteristics in the steady state are the same as those by the first definition.

In addition, it is found that the expressions for wave characteristics of the second order approximate solution of cnoidal wave theory by Chappellear using the second definition agree exactly with those by Laitone (1965), if the expansion

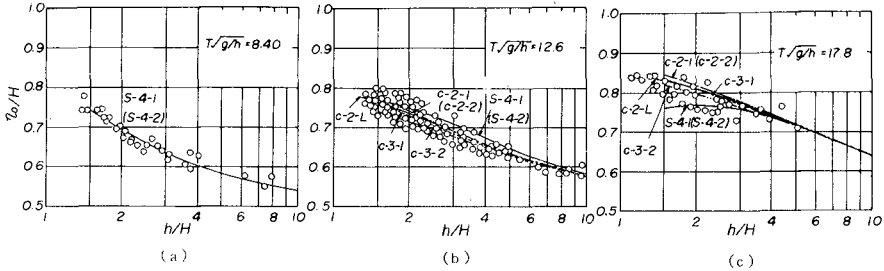


Fig. 2 Comparison for wave crest height above still water level

parameters  $L_0$  and  $L_3$  in the Chappellear theory are expanded into the power series of  $H/h$  and the expression is rewritten into the power series of the second order of  $H/h$  (Yamaguchi-Tsuchiya, 1974).

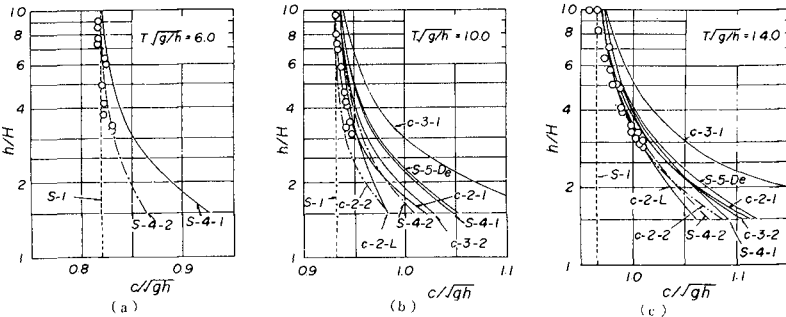


Fig. 3 Comparison for wave celerity (Experimental values shown were obtained by Iwagaki and Yamaguchi, 1967)

Figs. 2, 3 and 4 show the comparisons between the theoretical curves and the experimental results for wave crest height above the still water level, wave celerity and vertical distribution of horizontal water particle velocity at phase of wave crest respectively, in which  $\eta_0$  is the wave crest height above the still water level and  $T$  the wave period. In these figures, the notation S-1 indicates the theoretical curves for the Airy waves, S-4-1 and S-4-2 those for the Stokes waves of the fourth order approximation by the first and the second definition, S-5-De for the Stokes waves of the fifth order approximation by De (1955), c-2-1, c-2-2, c-3-1 and c-3-2 for the Chappellear cnoidal waves of the second and the third approximation by both the definitions, and c-2-L for the cnoidal waves of the second approximation by the second definition which Laitone (1965) converted from the depth below the wave trough to the mean water depth, respectively. The experimental results tend to agree more better with the theoretical curves by the second definition, although it is not capable of making clear enough which defini-

tion in the wave theory is more applicable for the estimation of horizontal water particle velocity, because of much scatter of the experimental values. It is however concluded from many examples of the comparison that the fourth order approximate solution of Stokes waves and the second one of cnoidal waves calculated using the second definition of wave celerity are more applicable for the estimation of wave characteristics. Therefore, these theories are used in the

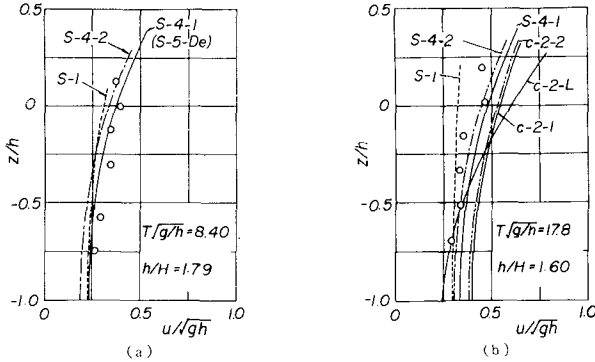


Fig. 4 Comparison for vertical distribution of horizontal water particle velocity at phase of wave crest

calculation of wave force in this paper.

(2) Wave Force Equation With the frame of reference shown in Fig. 5, the horizontal wave force  $dF$  on a segment  $dz$  of a pile can be expressed as

$$dF = \frac{\rho}{2} C_D A u |u| dz + \rho C_M V \frac{du}{dt} dz \dots (25)$$

in which  $\rho$  is the density of fluid,  $C_D$  the drag coefficient,  $C_M$  the inertia coefficient,  $du/dt$  the horizontal water particle acceleration,  $A$  the projected area perpendicular to the horizontal water particle velocity and  $V$  the displaced volume of the fluid. For a vertical circular cylindrical pile of the diameter  $D$ ,  $A$  and  $V$  are given by  $A = D$  and  $V = \pi D^2/4$  respectively. This is well-known as the Morison wave force equation (Morison, 1950). The first term indicates the drag force and the second the inertia force. Then, the total wave force is obtained by integrating Eq. (25) from the bottom to the water surface as

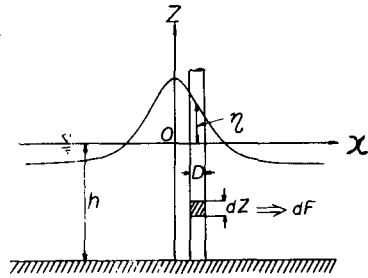


Fig. 5 Schematic diagram of wave force system used

$$F = \int_{-h}^{\eta} \frac{\rho}{2} C_D A u |u| dz + \int_{-h}^{\eta} \rho C_M V \frac{du}{dt} dz \dots (26)$$

The horizontal water particle acceleration by the Stokes waves using the second definition at phase of  $x = 0$  can be calculated by Eq. (18) as

$$\begin{aligned} \frac{du}{dt} = & -c\sigma \left[ \left\{ F_1 \cosh k(h+\eta) - F_0 F_1 \cosh k(h+\eta) - \frac{1}{2} F_1 F_2 \cosh 3k(h+\eta) \right\} \sin \sigma t + \left\{ 2F_2 \cosh 2k(h+\eta) \right. \right. \\ & - 2F_0 F_2 \cosh 2k(h+\eta) - \frac{1}{2} F_1^2 + F_1 F_3 \cosh 4k(h+\eta) \left. \right\} \sin 2\sigma t + \left\{ 3F_3 \cosh 3k(h+\eta) - \frac{3}{2} F_1 F_2 \right. \\ & \left. \left. \cosh k(h+\eta) \right\} \sin 3\sigma t + \left\{ 4F_4 \cosh 4k(h+\eta) - 2F_1 F_3 \cosh 2k(h+\eta) - F_2^2 \right\} \sin 4\sigma t \right] \dots (27) \end{aligned}$$

in which

$$F_0 = \lambda^2 A_{02} + \lambda^4 A_{04}, \quad F_1 = \lambda A_{11} + \lambda^3 A_{13}, \quad F_2 = 2(\lambda^2 A_{22} + \lambda^4 A_{24}), \quad F_3 = 3\lambda^3 A_{33}, \quad F_4 = 4\lambda^4 A_{44} \dots (28)$$

and  $\sigma (=2\pi/T)$  is the angular frequency.

If the inertia coefficient is assumed to be constant over a water depth, the total inertia force  $F_I$  is expressed by substituting Eq. (25) into the second term of Eq. (26) and integrating it from the bottom to the water surface as

$$F_I = -\rho C_M \nu \sigma^2 \left[ \left\{ F_1 \sinh k(h+\eta) - F_0 F_1 \sinh k(h+\eta) - \frac{1}{6} F_1 F_2 \sinh 3k(h+\eta) \right\} \sin \sigma t \right. \\ \left. + \left\{ F_2 \sinh 2k(h+\eta) - F_0 F_2 \sinh 2k(h+\eta) - \frac{1}{2} F_1^2 k(h+\eta) \right\} \sin 2\sigma t \right. \\ \left. - \frac{1}{4} F_1 F_3 \sinh 4k(h+\eta) \right] \sin 2\sigma t + \left\{ F_3 \sinh 3k(h+\eta) - \frac{3}{2} F_1 F_2 \sinh k(h+\eta) \right\} \sin 3\sigma t \\ \left. + \left\{ F_4 \sinh 4k(h+\eta) - F_1 F_3 \sinh 2k(h+\eta) - F_2^2 k(h+\eta) \right\} \sin 4\sigma t \right] \dots (29)$$

The total drag force  $F_D$  can be computed by integrating the following equation according to the Simpson rule, as the mathematical formulation for the total drag force is difficult.

$$F_D = \frac{\rho}{2} C_D A \int_{-h}^{\eta} u|u| dz \dots (30)$$

After all, the total wave force  $F$  is given as the sum of the drag force by Eq. (30) and the inertia force by Eq. (29).

$$F = F_D + F_I \dots (31)$$

On the contrary, if the second order approximate solution of cnoidal waves is used in place of the Stokes waves, the total inertia force can be written as

$$F_I = -\rho C_M \nu \frac{4K\sqrt{gh}}{T} h \left( 1 + \frac{\eta}{h} \right) \text{sn} \tau \text{cn} \tau \text{dn} \tau \left[ L_0 \kappa^2 + L_0^2 \kappa^2 (1 + \kappa^2) + 5L_0 L_3 \kappa^2 + 2L_0^2 \kappa^4 \text{sn}^2 \tau \right. \\ \left. + \frac{1}{2} \left\{ L_0^2 \kappa^2 (1 + \kappa^2) - 3L_0^2 \kappa^4 \text{sn}^2 \tau \right\} \left( 1 + \frac{\eta}{h} \right)^2 - \left( \frac{c}{\sqrt{gh}} \right)^{-1} \left\{ L_0^2 \kappa^2 \left( 1 - \frac{E}{K} \right) - L_0^2 \kappa^4 \text{sn}^2 \tau \right\} \right] \dots (32)$$

in which sn, cn and dn are the Jacobian elliptic functions with a real period and

$$\frac{\eta}{h} = 2L_3 + L_0(1 + \kappa^2) - L_0 \kappa^2 \text{sn}^2 \tau + L_3^2 + \frac{3}{20} L_0^2 (12 + 23\kappa^2 + 12\kappa^4) + 6L_0 L_3 (1 + \kappa^2) \\ - \frac{5}{2} L_0^2 \kappa^2 (1 + \kappa^2) \text{sn}^2 \tau - 6\kappa^2 L_0 L_3 \text{sn}^2 \tau + \frac{3}{4} L_0^2 \kappa^4 \text{sn}^4 \tau \\ \frac{c}{\sqrt{gh}} = 1 + L_3 + \left( 1 - \frac{E}{K} \right) \left\{ L_0 + (2 + \kappa^2 - \frac{E}{K}) L_0^2 + 5L_0 L_3 \right\}, \quad \tau = \frac{2K}{T} \dots (33)$$

The total drag force can be obtained by the similar numerical integration to the case of the Stokes waves described already.

(3) Estimation of Drag and Inertia Coefficients If the drag and inertia coefficients are assumed to be constant over a wave period and the vertical direction in water depth, they can be estimated respectively by the following equations using the experimental results of the time variations of total wave force and the corresponding water surface displacement. For the estimation of the drag coefficient, it can be expressed as

$$C_D = \frac{F_{\eta_0}}{(\rho/2) A \int_{-h}^{\eta_0} u|u| dz} \dots\dots\dots (34)$$

in which  $F_{\eta_0}$  is the total wave force measured at phase of wave crest.

Using the finite amplitude wave theories, the inertia force can not be separated from the total wave force unlike the method of estimation by the small amplitude wave theory, because the phase of zero points in the time variations of water surface displacement and horizontal water particle velocities does not coincide each other and the phase of the latter changes slightly with a location in water. Accordingly, for the estimation of the inertia coefficient, it can be expressed as

$$C_M = \frac{F_{\eta=0} - (\rho/2) C_D A \int_{-h}^0 u|u| dz}{\rho V \int_{-h}^0 (du/dt) dz} \dots\dots\dots (35)$$

in which  $F_{\eta=0}$  is the total wave force measured at phase of zero point in the time variation of water surface displacement.

Furthermore, for the representation of the drag coefficient, the Keulegan-Carpenter number (1958) which shows unsteadiness of wave motion is taken in addition to the wave Reynolds number. The Reynolds number  $Re$  and the Keulegan-Carpenter number  $KC$  are defined respectively as

$$Re = \frac{\sqrt{u_c^{2*}} D}{\nu} , \quad KC = \frac{\sqrt{u_c^{2*}} T}{D} \dots\dots\dots (36)$$

in which  $\nu$  is the kinematic viscosity and  $u_c^{2*}$  the averaged value of squared horizontal water particle velocity at phase of wave crest on an instantaneous water depth, which is also defined as

$$u_c^{2*} = \frac{\int_{-h}^{\eta_0} u^2 dz}{h + \eta_0} \dots\dots\dots (37)$$

CHARACTERISTICS OF DRAG AND INERTIA COEFFICIENTS

(1) Experimental Apparatus and Procedure The wave tank used in the experiment is 78 m long, 1.0 m wide and 1.5 m deep which has the sloping model beach of 1/100, 45 m long. The experimental apparatus is composed of the measurement system of wave force and a test pile set on the rigid frame at the location of about 53 m distance from the wave generator. The measurement system of wave force is to measure total wave force from the difference of the strain at two points on a pile generated by an action of waves. In the experiment, time variations of total wave force on a pile and surface displacement were measured in the wide range of wave characteristics. The wave characteristics used in the experiment are tabulated in Table 2. The previous experimental and observed results in addition to the experimental result of the authors are considered, as their outlines are shown in Table 3.

(2) Drag Coefficient Fig. 6 shows a relation between the drag coefficient and the wave Reynolds number. The coefficients were estimated by the fourth order approximate solution of Stokes waves as shown in Fig. 6 (a) and by the second approximate solution of cnoidal waves in Fig. 6 (b). In the figure, the experimental results by the authors, Goda, Burton et al., Jen and Ross and the observed ones by Morison et al. and Wiegel et al. are indicated. In the results by Ross and Morison et al., the maximum wave force was given only. However, the drag force was predominant taking into account of the wave-pile characteristics, so that the drag coefficient could be estimated from the maximum

Table 2 Wave characteristics used in experiment

Wave period T sec	Depth of water h cm	$T\sqrt{g/h}$	Diameter of pile D cm	Wave height H cm
1.5	55.6	6.30	14.0	9.3 - 37.5
1.5	55.6	6.30	28.0	12.4 - 34.2
2.0	55.6	8.40	14.0	7.8 - 40.9
2.0	55.6	8.40	21.0	6.6 - 33.4
2.0	55.6	8.40	28.0	6.9 - 40.7
2.5	55.6	10.5	14.0	5.4 - 43.2
2.5	55.6	10.5	21.0	5.6 - 36.6
2.5	55.6	10.5	28.0	7.7 - 47.6
3.0	55.6	12.6	7.0	4.9 - 44.2
3.0	55.6	12.6	14.0	4.7 - 46.9
3.0	55.6	12.6	21.0	4.5 - 37.4
3.0	55.6	12.6	28.0	4.7 - 46.9
2.5	27.8	14.8	7.0	5.3 - 23.6
2.5	27.8	14.8	14.0	4.9 - 23.6
3.0	27.8	17.8	7.0	4.2 - 21.2
2.6	41.7	12.6	7.0	5.5 - 31.6
1.8	14.0	12.6	7.0	5.0 - 12.7

Table 3 Outline of previous results of experiment and observation of wave force on a pile

Researcher	Year	Wave period T sec	Depth of water h cm	Wave height H cm	Diameter of pile D cm	Wave Reynolds number $Re \times 10^{-4}$
Morison et al.	1953	4.2 ~ 13.3	91.4 ~ 160.6	18.3 ~ 116.0	8.9	2.72 ~ 20.4
Haileman et al.	1955	1.0 ~ 1.49	30.5 ~ 124.1	12.2 ~ 25.6	1.27 ~ 15.2	0.48 ~ 8.1
Wiegel et al.	1957	9.1 ~ 18.6	1400.0 ~ 1500.0	134.2 ~ 625.0	32.4, 61.0	19.0 ~ 130.0
Ross	1959	3.75 ~ 16.0	153.0 ~ 458.0	58.0 ~ 235.0	32.4	21.0 ~ 86.0
Goda	1964	1.37 ~ 7.96	100.0, 130.0	9.3 ~ 80.1	7.6, 14.0	1.43 ~ 21.8
Jen	1967	0.91 ~ 5.30	91.4	2.1 ~ 18.3	15.2	0.38 ~ 5.7
Burton et al.	1970	0.81 ~ 1.67	61.0	1.0 ~ 25.4	9.4 ~ 10.2	0.67 ~ 5.1

wave force. Also, the drag coefficients by the authors, Jen and Burton et al. are limited in the case where the drag force is more than about 15 % of the maximum total wave force. The curves shown in the figure are the drag coefficient in a uniform flow by Vennard, Goldstein and Fage et al. respectively which differs each other corresponding to the extent of turbulence intensity near the critical Reynolds number. There is hardly prominent difference on the whole trend between the results by the Stokes waves and those by the cnoidal waves. It is found from the figure, in spite of large scatter of the results that the drag coefficient tends to decrease with the increase of the wave Reynolds number in the ranges of  $Re < 2 \times 10^5$  and  $Re > 10^5$ . Accordingly, the drag coefficient is considerably different at the same Reynolds number. This may be not only due to the scatter caused by experimental error but also due to the dependence on the other parameter affecting the drag coefficient of a pile in wave motion, in addition to the wave

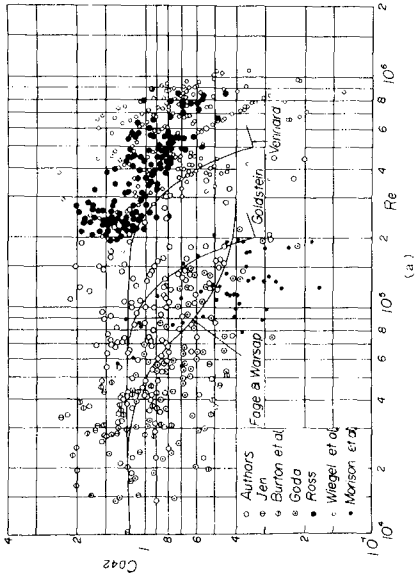
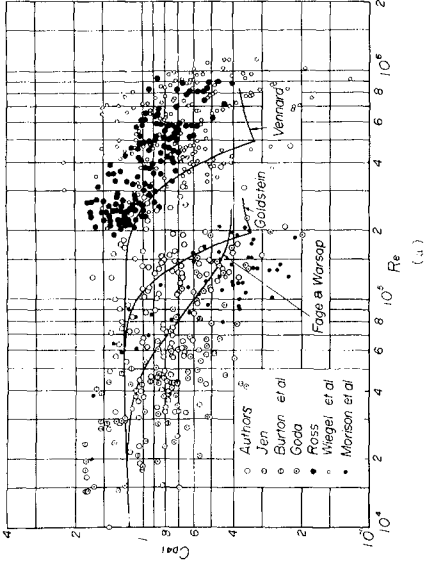


Fig. 6 Relation between drag coefficient and wave Reynolds number (1)

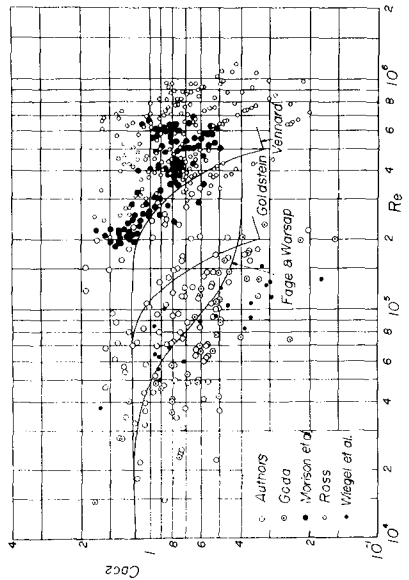
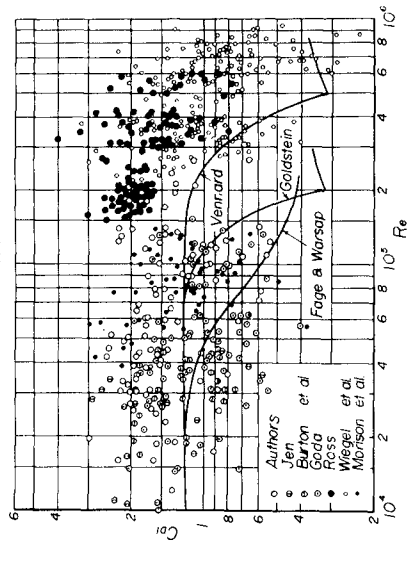
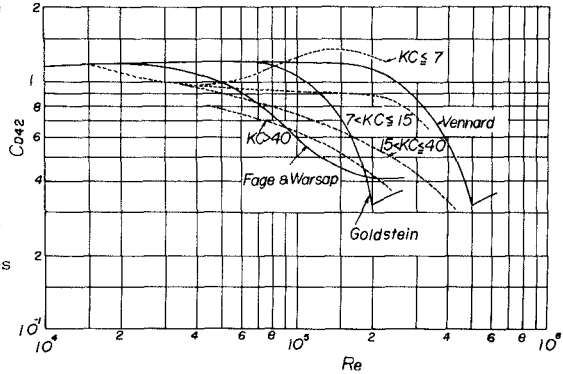


Fig. 7 Relation between drag coefficient and wave Reynolds number (2)

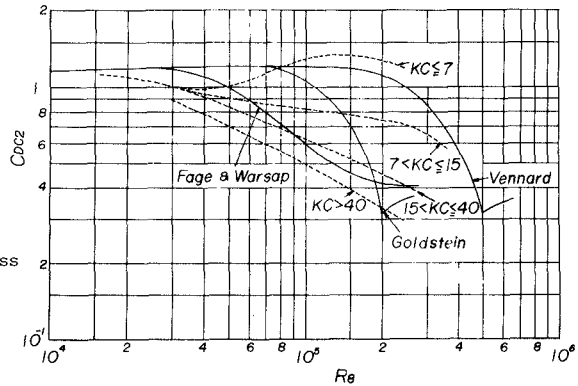
Reynolds number.

Fig. 7 shows the similar results to Fig. 6, in the case where the fourth order approximate solution of the Stokes wave theory by the first definition and the Airy wave theory were used. In this figure, the drag coefficient  $C_{D1}$  was obtained by the Stokes wave theory and  $C_{D1}$  by the Airy wave theory. The drag coefficient estimated using the Stokes wave theory by the first definition becomes slightly smaller than the one by the second definition and there is little difference in the relation with the wave Reynolds number. On the contrary, the drag coefficient by the Airy wave theory is larger than the results by the finite amplitude wave theories and the range of scatter is wider, because the wave crest height above the still water level and the horizontal water particle velocity are underestimated.

The Keulegan-Carpenter number is well-known as one of the dimensionless parameters to be described the unsteadiness of wave motion. Figs. 8 and 9 are the drag coefficient described in relation to the wave Reynolds number and the Keulegan-Carpenter number. The curve indicated by broken line was obtained being classified the data into some intervals of the wave Reynolds number and averaged. Although the experimental values of drag coefficient are scattered as shown in Figs. 6 and 7, the drag coefficient at a constant wave Reynolds number generally decreases with the increase of the Keulegan-Carpenter number. It is supposed referring to the Bidde (1970) experiment that the reason can be explained as; the trend in the small value of the Keulegan-Carpenter number approaches the Vennard curve in a uniform flow with small turbulence intensity and the trend in large value corresponds to the Fage and Warsap curve in a uniform flow with large turbulence



(a)



(b)

Fig. 8 Relation between drag coefficient and wave Reynolds number with Keulegan-Carpenter number (1)

intensity. There is similar trend in the relation between the drag coefficient estimated by the cnoidal waves and the above parameters.

(3) Inertia Coefficient  
 Fig. 10 is a relation between the inertia coefficient and the ratio of wave height to pile diameter. The upper figure was obtained using the Stokes wave theory by the second definition and the lower by the cnoidal waves. The curve shows a general trend obtained by averaging experimental values. The coefficient by both the theories tends to decrease slightly with the increase of the ratio, except for the observed values by Wiegel et al. (1957). The increase of the ratio means the increase of drag force in the total wave force. Therefore, this may be due to the vortex shedding behind the pile in the predominant region of drag force, according to the Sarpkaya and Garrison (1963) study on the inertia coefficient of a pile in a unidirectional accelerated flow.

Fig. 11 is also the similar relation. The wave theories used in the estimation of the coefficient are the Stokes wave theory by the first definition of which result is shown in Fig. 11(a) and the Airy wave theory in Fig. 11(b), respectively. It is clear from the comparison between Figs. 10 and 11 that there is hardly prominent influence of wave nonlinearity on the inertia coefficient, because the inertia coefficient is changed nothing but slightly larger than the one by the finite amplitude wave theories.

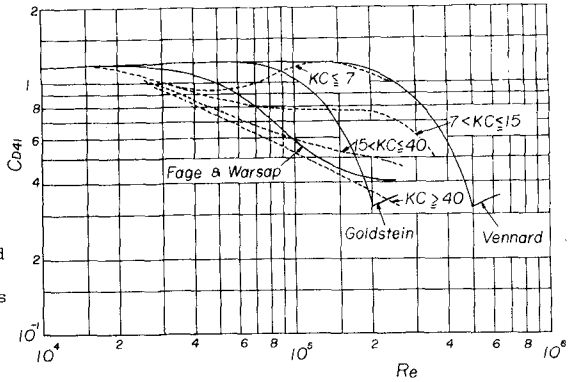


Fig. 9 Relation between drag coefficient and wave Reynolds number with Keulegan-Carpenter number (2)

TOTAL WAVE FORCE

(1) Time Variations of Total Wave Force  
 Keulegan and Carpenter (1958) estimated the phase variation of the drag and inertia coefficients from the results of experiment of wave force on a horizontal circular pile using the Airy wave theory. In so far as the finite amplitude wave theories are used, however, such an analysis is so difficult that the effect of the phase variation of the coefficients on the time variation of total wave force is investigated from comparison between the theoretical curves and the experimental results of the time variation of total wave force. In this case, the coefficients are assumed to be constant over a wave period.

Some examples of the comparison are shown in Fig. 12 of which the upper figure is the corresponding time variation in the water surface displacement. In this figure, the solid line indicates the theoretical total wave force by the Stokes waves, the two-dotted chain line the one by the cnoidal waves and the broken line and the one-dotted chain line indicate respectively the theoretical drag and inertia force by the Stokes waves. The coefficients in themselves estimated directly from the experimental results by the method mentioned previously were used in the theoretical computation of total wave force. The experimental

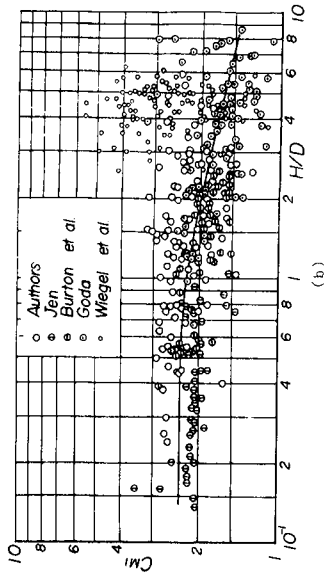
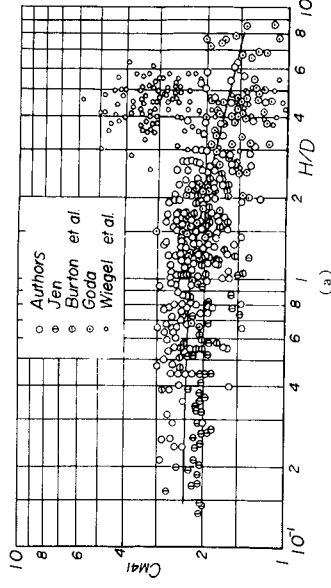


Fig. 11 Relation between inertia coefficient and ratio of wave height to pile diameter (2)

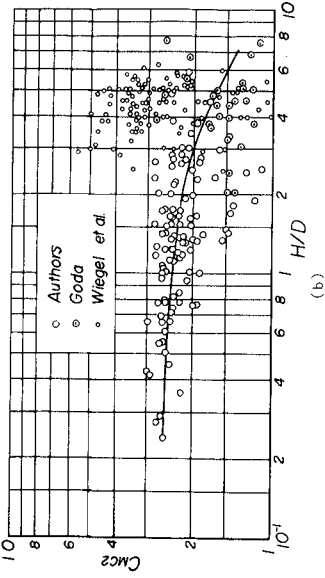
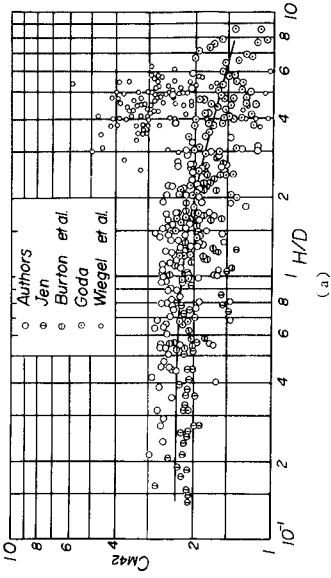


Fig. 10 Relation between inertia coefficient and ratio of wave height to pile diameter (1)

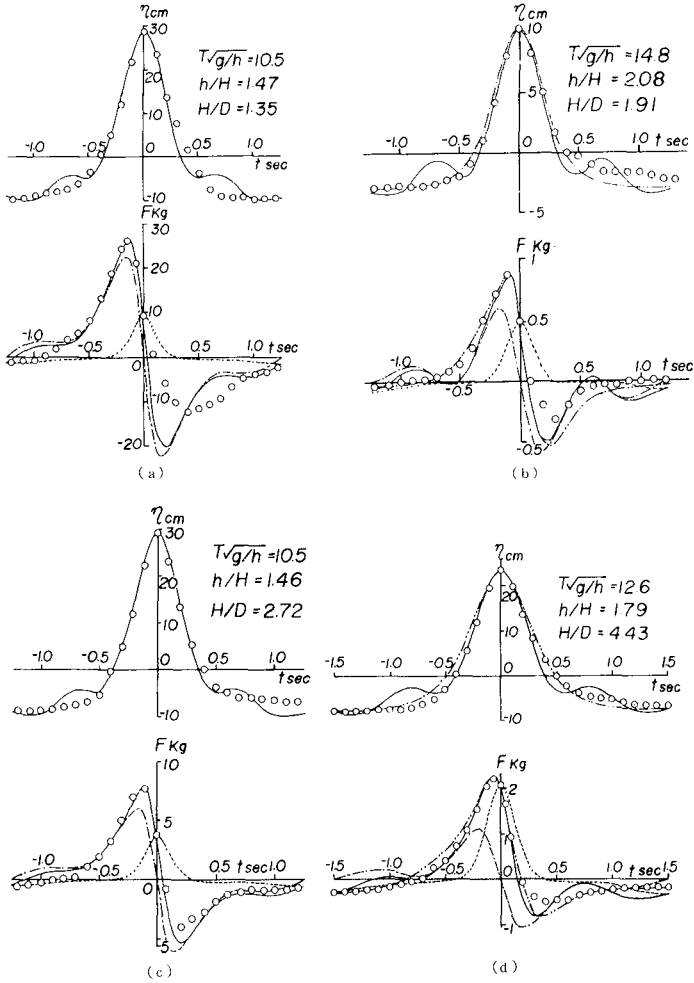


Fig. 12 Time variations of water surface displacement and total wave force in comparison with theories

time variation of total wave force and the corresponding water surface displacement agree well with the theoretical curves by the Stokes waves within the range of  $T\sqrt{g/h} \leq 12.6$  and those by the cnoidal waves within the range of  $T\sqrt{g/h} \geq 14.8$ . From the above consideration, it is expected that the phase variation of the coefficients has not so serious effect on the computed results of total wave force.

Fig. 13 is another comparison of the time variation of total wave force. In this figure, the solid line indicates the theoretical total wave force including the effect of the convective term in water particle acceleration and the broken line the one not including the convective term. The influence of the convective term on the total wave force is only a few percent at most, but it would affect the maximum total wave force when the inertia force becomes predominant.

(2) Maximum Total Wave Force The applicability of the total wave force equation by finite amplitude wave theories to the estimation of maximum total wave force is investigated. In this case, the wave theories used are such as the Airy wave, Stokes wave and cnoidal wave theories explained already.

Fig. 14 shows one of the comparisons, where the abscissa gives the measured wave force or bottom moment and the ordinate is the computed one. In this figure, the fourth order approximate solution of the Stokes waves by the second definition of wave celerity, the one by the first definition and the cnoidal wave theory were used respectively with the constant drag and inertia coefficients. There is relatively good correspondence between them, except for the experimental values by Goda (1964), in which the computed results show larger values than the experimental ones, because the drag force is predominant in the most of his experiment and moreover the estimated drag coefficient is smaller than 1.0 in most cases. Taking into account of the poor correspondence between the theoretical results applying the Airy wave theory and the experimental ones, as shown in Fig. 15, the results mentioned above describe the good efficiency of the wave force equation applying the finite amplitude wave theories and the appropriateness of selected values of the coefficients in practical purposes.

The comparison in the case where both the drag and inertia coefficients were estimated respectively from the relations proposed by the authors is shown in Fig. 16. Although there are some cases where the correspondence becomes poorer in comparison with Fig. 14, if the inertia coefficient is determined from the relations proposed, the mutual correspondence becomes better and the range of scatter narrower in general cases. It may be worthwhile recommending from the

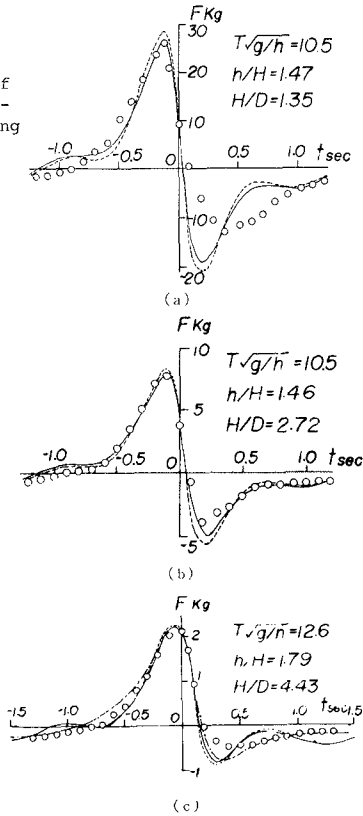


Fig. 13 Influence of convective term in water particle acceleration on total wave force

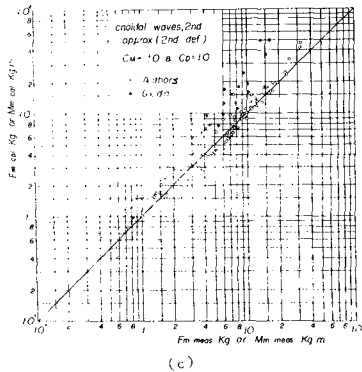
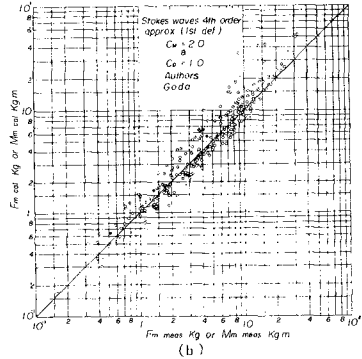
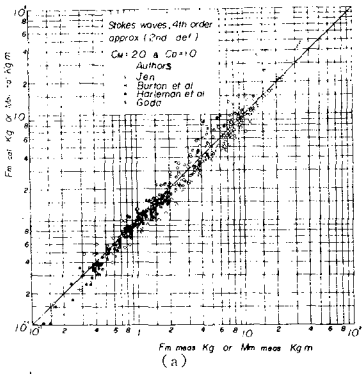


Fig. 14 Comparison between experimental and computed maximum total wave forces (1)

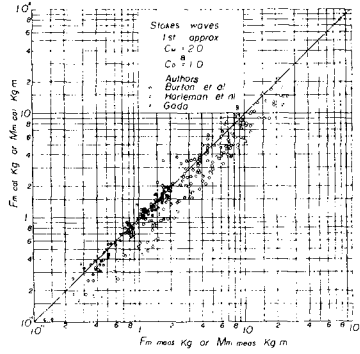


Fig. 15 Comparison between experimental and computed maximum total wave forces (2)

above consideration that the estimation of wave force on a pile by such a method is more hopeful.

CONCLUSIONS

The Stokes wave theory of the fourth order approximation by Skjelbreia and Hendrickson and the cnoidal wave theory of the third approximation by Chappelare were recalculated using the Stokes second definition of wave celerity and it was found from the comparison with the experimental results that these theories are more applicable for the estimation of wave characteristics.

The theories were applied to the wave force equation by Morison and the drag and inertia coefficients were estimated from many experimental results including the previous studies of wave force on a pile. As a result, relations between the drag and inertia coefficients and the wave-pile characteristics were established respectively.

It was shown that the wave force equation using either the Stokes wave theory or the cnoidal wave theory and the drag and inertia coefficients proposed, is very effective to estimate the maximum total wave force on a pile due to finite amplitude but nonbreaking waves.

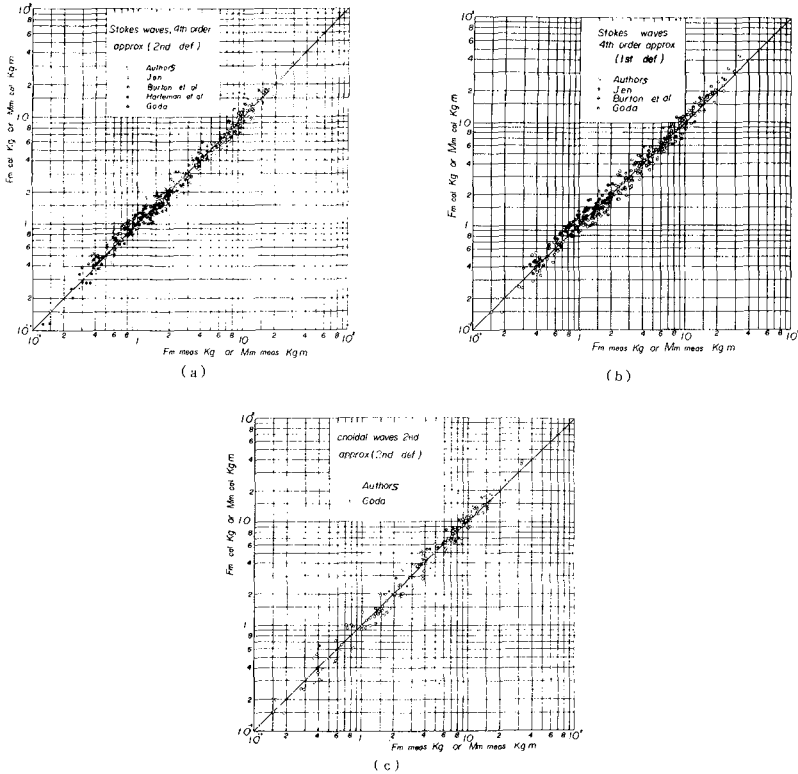


Fig. 16 Comparison between experimental and computed maximum total wave forces (3)

Although a practical method was proposed for the estimation of total wave force on a vertical circular cylindrical pile within the range of experiment, further investigations should be carried out for the range of higher wave Reynolds number.

#### ACKNOWLEDGEMENTS

Part of this investigation was accomplished with the support of the Science Research Fund of the Ministry of Education, for which the authors express their appreciation. Thanks are due to Mr. T. Shibano, Research Assistant, Disaster Prevention Research Institute, Kyoto University, for his kind help in preparing this paper.

## REFERENCES

- Bidde, D. D. (1970). Wave Forces on a Circular Pile Due to Eddy Shedding, Univ. of California, Berkeley, Hydraulic Engg. Laboratory, Tech. Report, HEL 9-16, pp. 1-141.
- Burton, W. J. and Sorensen, R. M. (1970). The Effects of Surface Roughness on the Wave Forces on a Circular Cylindrical Pile, Texas A & M Univ., COE Report, No. 121, pp. 1-37.
- Chappellear, J. E. (1962). Shallow-Water Waves, Jour. Geophys. Res., Vol. 67, No. 12, pp. 4693-4704.
- De, S. C. (1955). Contributions to the Theory of Stokes Waves, Proc. Cambridge Phil. Soc., No. 51, pp. 713-736.
- Goda, Y. (1964). Wave Forces on a Vertical Circular Cylinder; Experiments and a Proposed Method of Wave Force Computation, Report of Port & Harbour Tech. Res. Inst., No. 8, pp. 1-74.
- Harleman, D. R. F. and Shapiro, W. C. (1955). Experimental and Analytical Studies of Wave Forces on Offshore Structure, Part 1, MIT Hydrodynamics Laboratory, Tech. Report, No. 19, pp. 1-55.
- Iwagaki, Y. and Yamaguchi, M. (1967). On the Limiting Condition of Stokes Waves and Cnoidal Waves, Proc. 14th Conf. on Coastal Engg., JSCE, pp. 8-16(in Japanese).
- Jen, Y. (1967). Wave Forces on Circular Cylindrical Piles Used in Coastal Structure, Univ. of California, Berkeley, Hydraulic Engg. Laboratory, Tech. Report, HEL 9-11, pp. 1-94.
- Keulegan, G. H. and Carpenter, L. H. (1958). Forces on Cylinders and Plates in an Oscillating Fluid, Jour. Res. NBS, Vol. 60, No. 5, pp. 423-440.
- Laitone, E. V. (1961). The Second Approximation to Cnoidal and Solitary Waves, Jour. Fluid Mech., Vol. 9, pp. 430-444.
- Laitone, E. V. (1965). Series Solutions for Shallow Water Waves, Jour. Geophys. Res., Vol. 70, No. 4, pp. 995-998.
- MacCamy, R. C. and Fuchs, R. A. (1954). Wave Forces on Piles; A Diffraction Theory, Tech. Memo. BEB, No. 69, pp. 1-17.
- Morison, J. R. (1950). Design of Piling, Proc. 1st Conf. on Coastal Engg., pp. 254-258.
- Morison, J. R., Johnson, J. W. and O'Brien, M. P. (1953). Experimental Studies of Forces on Piles, Proc. 4th Conf. on Coastal Engg., pp. 340-370.
- Ross, C. W. (1959). Large-Scale Tests of Wave Forces on Piling, Tech. Memo. BEB, No. 111, pp. 1-9.
- Sarpkaya, T. and Garrison, C. J. (1963). Vortex Formation and Resistance in Unsteady Flow, Jour. Applied Mech., Vol. 30, No. 1, pp. 16-24.
- Skjelbreia, L. and Hendrickson, J. A. (1960). Fifth Order Gravity Wave Theory, Proc. 7th Conf. on Coastal Engg., pp. 184-197.
- Stokes, G. G. (1880). On the Theory of Oscillatory Waves, Math. Phys. Paper, Vol. 8, pp. 197-229.
- Tsuchiya, Y. and Yamaguchi, M. (1972). Some Considerations on Water Particle Velocities of Finite Amplitude Wave Theories, Coastal Engg. in Japan, Vol. 15, pp. 43-57.
- Wiegel, R. L., Beebe, K. E. and Moon, J. (1957). Ocean Wave Forces on Circular Cylindrical Piles, Proc. ASCE, Vol. 83, HY2, pp. 89-119.
- Yamaguchi, M. and Tsuchiya, Y. (1974). Nonlinear Effect of Waves on Wave Pressure and Wave Force on a Large Cylindrical Pile, Proc. JSCE, No. 229, pp. 151-163(in Japanese).
- Yamaguchi, M. and Tsuchiya, Y. (1974). Relation between Wave Characteristics of Cnoidal Wave Theory Derived by Laitone and by Chappellear, Bull. DPRI, Kyoto Univ., Vol. 24, Part 3(in preparation).